On the interplay between the heartbeat oscillations and wind outflow in the microquasar IGR J17091-3624

Mikołaj Grzędzielski

Center for Theoretical Physics Polish Academy of Sciences

19th November 2014

Collaboration

- Agnieszka Janiuk (Centrum Fizyki Teoretycznej PAN)
- Fiamma Capitanio (INAF-Instituto di Astrofisica e Planetologia Spaziali, Rome, Italy)
- Stefano Bianchi (Dipartimento di Matematica e Fisica, Università degli Studi Roma Tre,Rome, Italy)

Schedule

Schedule

- X-Ray binaries
- IGR-J-17091
- Model of accretion disk
- Observational data
- Comparison model-data
- Discussion and conclusions

Cygnus X-1

- First known black hole candidate, discovered by Uhuru X-Ray Satellite/ X-ray Explorer Satellite, SAS-A in 1971
- High-mass X-ray binary system about 6,070 light-years from the Sun that includes a blue supergiant variable star $M = 20 M_{\odot}$
- X-ray spectrum of Cygnus X-1 can be characterized as a power law of the photon index γ 1.5 – 1.9 (Liang Nolan 1984)
- Hard and soft states

GRS 1915+105

- Discover in 1992 by the satellite GRANAT
- Pseudo-superluminal jet expansion (Yadav et. al. 2006)
- Hearbeat variability(Neilsen et. al. 2011)

Microquasar IGR-J-17091-3624

- Heartbeat at the period between 5 and 70 seconds - possible by radiation pressure instability
- Moderately bright transient X-ray binary
- Peak flux level at 20 mCrab in the range $20 - 100$ keV
- Discovered by INTEGRAL/IBIS in 2003 (Kuulkers et. al. Astron. Telegram. 149)
- Was searched in archival data of previous missions (TTM-Kvant,BeppoSAX)

Microquasar IGR-J-17091-3624

- Refined position of $IGR - J - 17091 - 3624$ provided by Kennea Capitani (2007)
- At the end of January 2011 Swift/BAT reported renewed activity of IGR-J-17091; 28 February 2011 started a long monitoring campaign
- 2011 outbursts increased to 120 mCrab (brightest outburst even observed from that object)
- *RXTE*/PCA data showed a continous progression
- IGR-J-17091-3624 presents fast and ionized wind observed during the soft spectral state
- Similarities between IGR-J-17091-3624 and GRS-1915+105 - quasi periodic flare-like events at frequency 25-30 mHz (Altamirano et. al. 2011b, 2011c)

Microquasar IGR-J-17091-3624 - size of distance

- Binary object with black hole at mass $6M_{\odot}$ (Rebusco et. al. (2012))
- Distance - more than 22 kpc ($6.6 \cdot 10^{22} cm$) (D. Altamirano et. al)
- Radius of accretion disk - $R_{max} = 7.05 \times 10^{10} - 2.38 \times 10^{11}$ - estimation from orbital period measures (Wijnands et.al (2012))

IGR-J-17091 and GRS-1915 lightcurves - comparison

The upper and lower panels of each frame show a light curve of IGR J17091–3624 and GRS 1915+105, respectively. Count rates are given in 1 s bins, per PCU, 2-60 keV and background subtracted (Altamirano et. al. 2012)

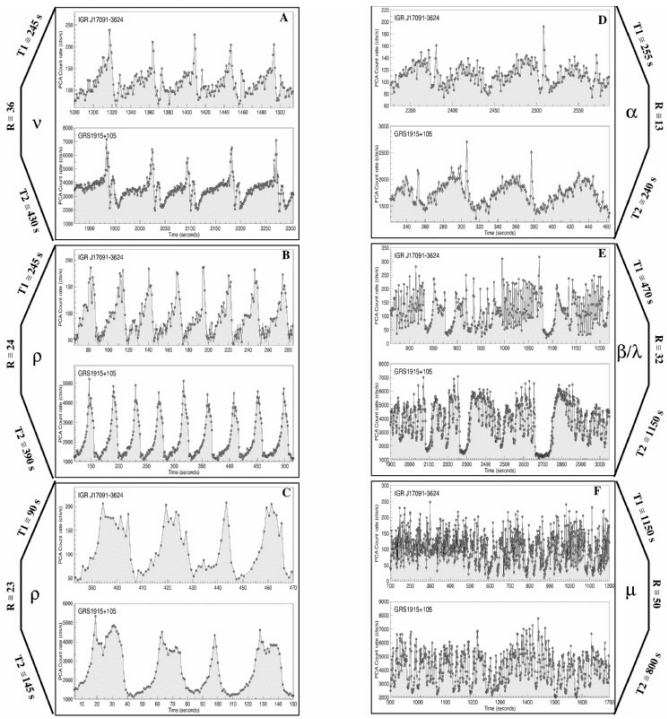

Our model

Our model - GLADIS code

- GLADIS Code - 1.5 D - model - approaching in
- radiation pressure instability
- α - disk.
- non-diagonal term of the stress tensor $T_{r\phi}$ proportional to total (gas + radiation) pressure P (Shakura & Sunyaev)

$$T_{r\phi} = -\alpha p \tag{1}$$

Physics of the model

We assumed the non-diagonal terms in stress tensor in cylindrical coordinates proportional to the total pressure with a constant viscosity α, as introduced by (Shakura, Sunyaev (1973))

$$T_{r\phi} = -\alpha P, \tag{2}$$

where P is pressure.
If we consider a thin disk that has an energy loss connected only with horizontal flows, local energy loss in the disk per unit volume per unit time is given by:

$$\frac{\partial F}{\partial z} = T_{r\phi}\partial_r v_\phi \tag{3}$$

Physics of the model-dimensionless accretion rate

and the dimensionless accretion rate is

$$\dot{m} = \frac{\eta \dot{M} c^2}{L_{Edd}} = \frac{\dot{M}}{\dot{M}_{Edd}} \tag{4}$$

Here η is efficieny of accretion, equal to $1/16$ in the pseudo-Newtonian approximation. The final formula for the viscous energy dissipation is:

$$\frac{\partial F_{tot}}{\partial z} = \alpha P \partial_r v_\phi \tag{5}$$

Physics of the model - pressure

The equilibrum pressure consists of gas and radiation pressure

$$P = P_{\rm gas} + P_{\rm rad} \tag{6}$$

where we assume that gas is an ideal gas of protons of mass m_p

$$P_{\rm gas} = \frac{\rho k_B}{m_p} T \tag{7}$$

and the radiation pressure is given by

$$P_{\rm rad} = \frac{4\sigma_B}{3c} T^4 \tag{8}$$

Stationary case

We consider here the model of vertically averaged disk (effectively, 1.5-dimensional model, as the motion in the angular direction is also accounted for). In the simpliest possible stationary case, we close the equations by an energy conservation equation

$$F_{\rm tot} = Q_+ = Q_- \tag{9}$$

where the total flux locally emitted from the surface of the accretion disk is given by the global parameters:

$$F_{\rm tot} = \frac{3GM\dot{M}}{8\pi r^3} f(r) \tag{10}$$

Heat equilibrum

where $f(r)$ is given by the boundary condition on the inner edge of accretion disk. The vertically averaged viscous heating rate in the disk is

$$Q_+ = \frac{3}{2}\alpha P H \Omega_K \tag{11}$$

and the radiative cooling rate per unit time per surface unit is

$$Q_- = \frac{4\sigma_B T^4}{3\kappa\Sigma}. \tag{12}$$

where κ is the electron scattering opacity which equal to 0.34 $\mathrm{cm}^{-2}\ \mathrm{g}^{-1}$.

Physics of the model - possibility of outburst

- The outbursts of accretion disks may be induced by the two main types of instabilities which lead to the thermal-viscous oscillations - radiation pressure instability and ionization instability - more discussed in (Janiuk, Czerny 2011)
- In our model we assume disk with radiation pressure which may leads to radiation pressure instability
- For our parameters disk is stable for $\dot{m} > 0.036$

1.5 D hydrodynamics - mass, angular momentum and energy conservation

In the time-dependent model we solve the full set of equations of hydrodynamics. We consider a model of thin disk, so in the conservation of mass (continuity) equation we neglect z-behaviour of density and velocity fields:

$$\frac{\partial(\Sigma v_r)}{\partial r} + r\frac{\partial \Sigma}{\partial t} = 0 \tag{13}$$

The mass conservation equation is

$$\frac{\partial \Sigma}{\partial t} = \frac{1}{2\pi r}\frac{\partial(-2\pi r \Sigma v_r)}{\partial r} \tag{14}$$

The angular momentum conservation is included in following equation

$$\dot{M}\frac{d}{dr}(r^2\Omega) = -\frac{\partial}{\partial r}(2\pi r^2 T_{r\phi}) \tag{15}$$

We define ν as the kinematic viscosity $T_{r\phi} = \alpha PH = (3/2)\Omega\nu\Sigma$

Full set of equations

From mass and angular momentum conservation equations (14,15) and the kinematic viscosity definition we obtain the final formula on the evolution of the surface density of disk (Janiuk, Czerny 2002):

$$\frac{\partial \Sigma}{\partial t} = \frac{1}{r}\frac{\partial}{\partial r}(3r^{1/2}\frac{\partial}{\partial r}(r^{1/2})\nu\Sigma) \tag{16}$$

$$v_r = -\frac{3}{\Sigma}r^{-1/2}\frac{\partial}{\partial r}(\nu\Sigma r^{1/2}) \tag{17}$$

We also have the energy conservation equation (Janiuk, Czerny 2002)

$$\frac{\partial \ln T}{\partial t} + v_r\frac{\partial \ln T}{\partial \ln r} = \frac{4-3\beta}{12-10.5\beta}(\frac{\partial \ln \Sigma}{\partial \ln r} - \frac{\partial \ln H}{\partial \ln r} + v_r\frac{\partial \ln \Sigma}{\partial \ln r}) + \frac{Q_+ - Q_-}{(12-10.5\beta)PH} \tag{18}$$

Wind

The mass loss rate (propably in the verical direction is equal to the ratio of the locally generated flux in the accretion disk, with a fraction determined by f_{out}, to the energy change per particle, $\dot{m}_z = F_{tot}(1 - f_{out})/(\Delta E/m_p)$. The local flux is given by the Equation 10 of the standard accretion disk theory

$$f_{out} = 1 - \frac{1}{(1 + A\dot{m}^2)} \tag{19}$$

Wind

We assume that this relation holds also in the hydrodynamical computations. The energy change per particle is on the order of virial energy, $\Delta E = BkT_{vir} = BGM/r$, with $B \sim 1$, so expressing the mass loss rate in terms of local variables, in the units of [g s^{-1} cm^{-}2], we have a final formula:

$$\dot{m}_z(r) = B\frac{3}{4}\frac{1}{r}\Sigma v_r f(r) f_{out} \tag{20}$$

with f_{out} given by Equation 19.

Wind - general picture

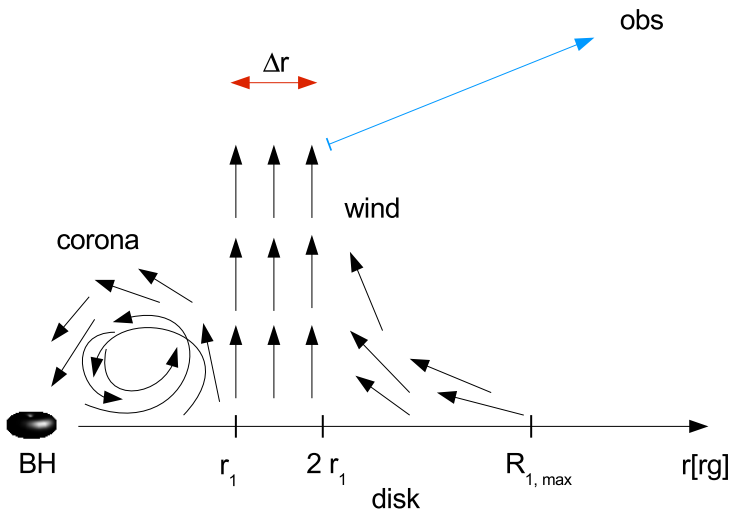

Figure: *Chandra* ACIS-S HETG spectra for observation 12406 (*upper panel*) and 12405 (*lower panel)* in the 6-7.5 keV energy range. The wind components observed in observation 12406 are completely undetectable in observation 12405, if we assume that the wind density is a factor of 10 lower

Wind - general picture

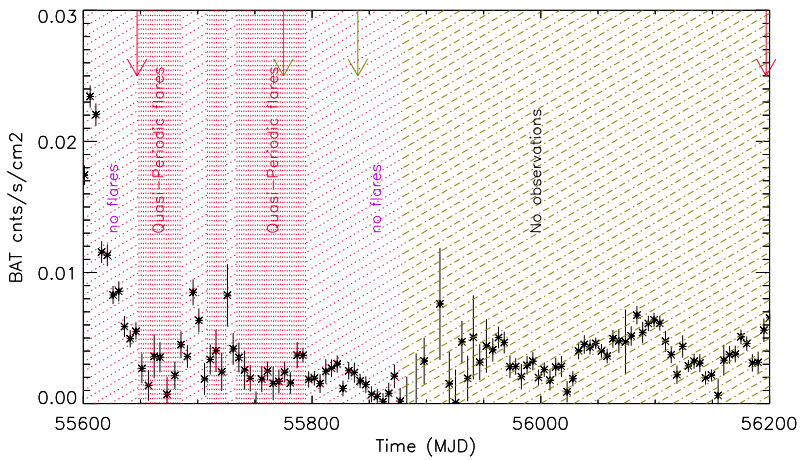

Figure: The time-line sketch created from the *Swift*/XRT and *RXTE*/PCA data analysis, showing the correlation of the wind and heartbeat presence in IGR J17091, superimposed to the *Swift*/BAT 15-50 keV light curve. The second *Chandra* observation (second green arrow) shows a fast, ionized wind, while the first *XMM-Newton* observation (first red arrows) and the first *Chandra* observation (first green arrow) lie in the heartbeat zone and does not show any detectable wind outflow. During the last *XMM-Newton* observation, the source is in hard state.

Obtaining the observational data

- SWIFT mission
- X-Ray data from termal radiation of the disk - XRT
- 0.2 – 10 keV
- FITS files archives
- HEASOFT - High Energy Astrophysics SOFTware v.6.15
- XRT pipeline
- XSELECT extracting

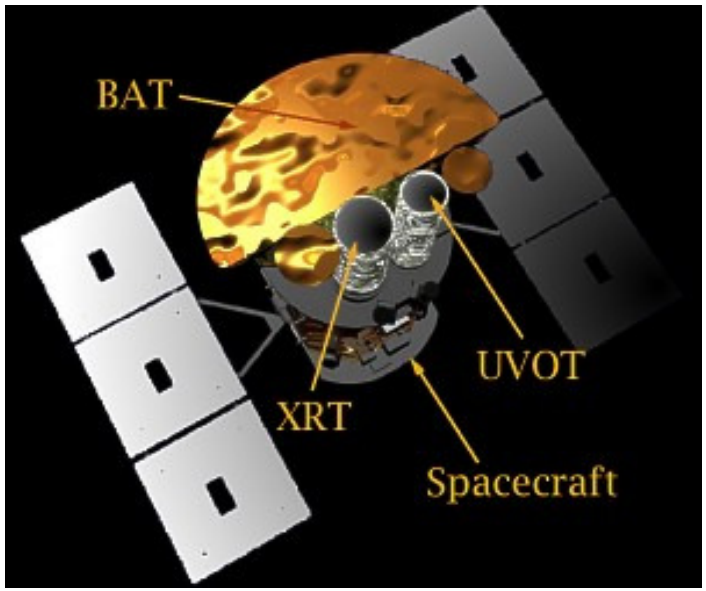

Observational data

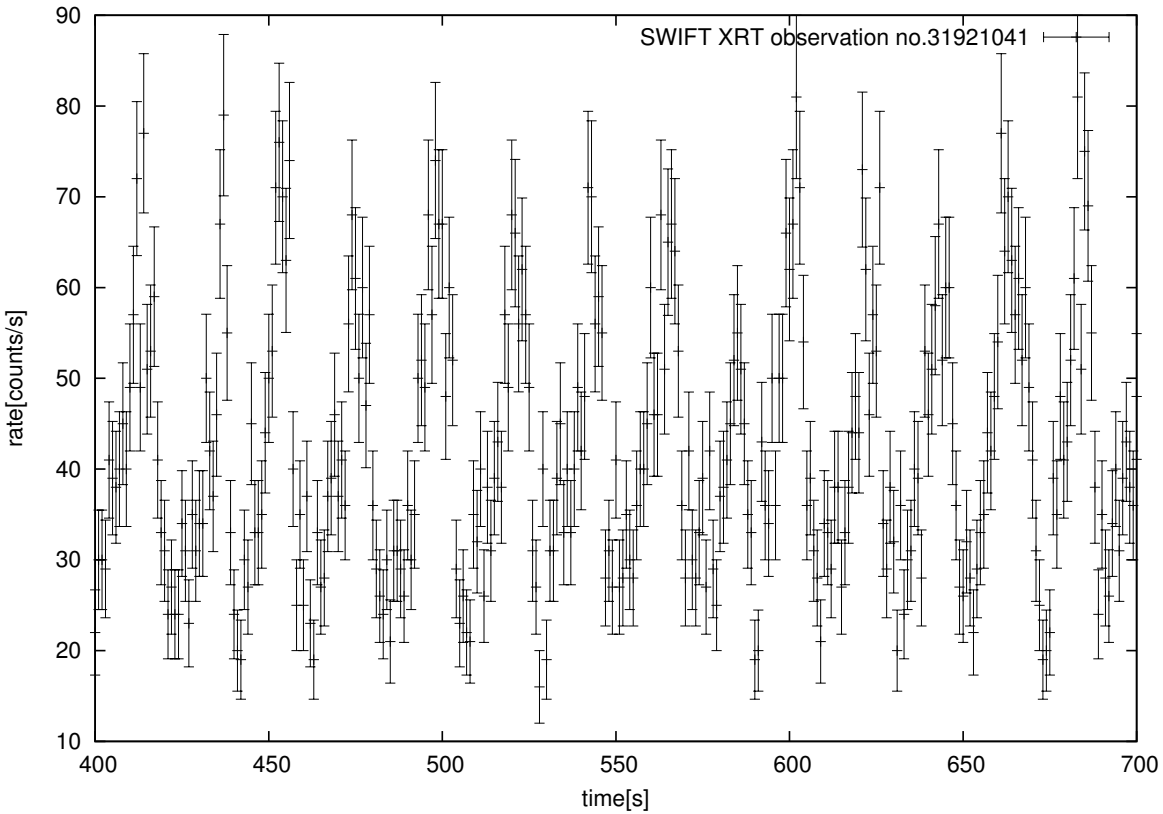

Photoionization modeling

- In order to characterise the wind in the *Chandra* observations, we prepared two tables with the photoionization code Cloudy C13.02
- From the best fit values of the ionization parameter $\xi = \mathrm{L_{ion}}/\mathrm{nr}^2$, assuming the $\mathrm{L_{ion}} = 3.7 \times 10^{37}$ erg s^{-1}, we get $n_1 r_1^2 \simeq 1.5 \times 10^{34}$ and $n_2 r_2^2 \simeq 5.8 \times 10^{33}$ cm^{-1} for the two wind components, respectively. The corresponding (spherical) mass outflow rates would be

$$\dot{M}_{wind} \simeq 1.23 m_p f v \Omega n r^2 \tag{21}$$

where m_p is the proton mass (the 1.23 correction factor comes from assuming cosmic elemental abundances), Ω is the covering factor and f the filling factor. The absence of emission lines suggests $\Omega/4\pi \simeq 0.5$ 2012ApJ...746L..20K, so our estimated mass outflow rates are:

$$\dot{M}_{wind1} \simeq 1.8 \times 10^{20}\, f_1 \ \mathrm{g\,s^{-1}} \tag{22}$$

$$\dot{M}_{wind2} \simeq 1.2 \times 10^{20}\, f_2 \ \mathrm{g\,s^{-1}} \tag{23}$$

Photoionization modeling

- Filling factors f_1 and f_2 are difficult to estimate
- We can assume that extension of wind is comparable to launching radius and we have $N_H = fnr$
- It leads to $r_1 \simeq 1900 r_g$ and $r_2 \simeq 760 r_g$ correspondig to $n_1 \simeq 5.1 \times 10^{15}$ cm^{-3}
- Resulting filling factors are $f_1 \simeq 0.0015$ and $f_2 \simeq 0.0037$
- Resulting wind components $\dot{M}_{wind1} = 2.7 \times 10^{17}$ and 4.2×10^{17} and $\dot{M}_{wind2} = 2.7 \times 10^{17}$ and 4.2×10^{17}

- For $\dot{M} > 0.04$ radiation pressure instalibity lead to outbursts

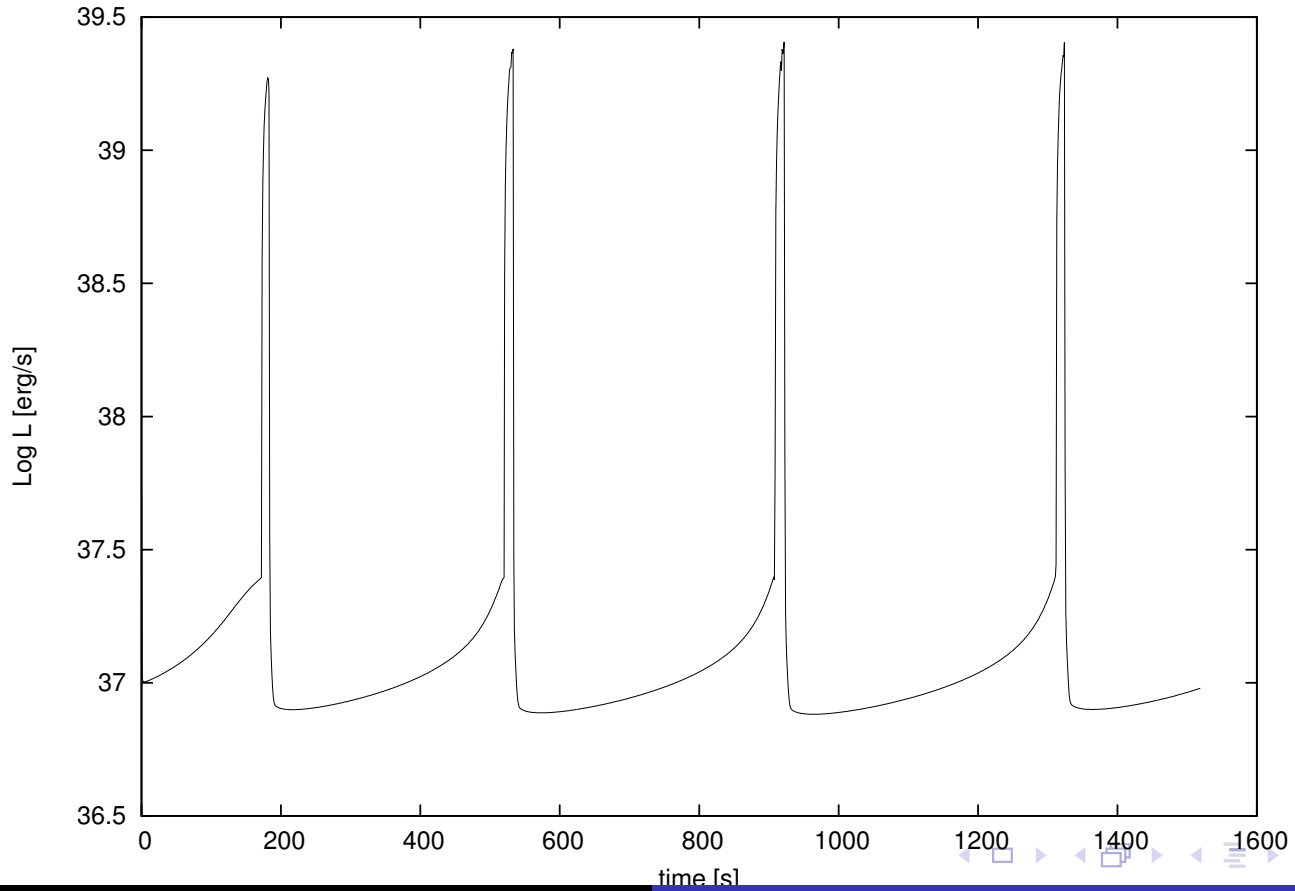

Regularity and grid

N_p	period	error	variance	duration of outburst	error	variance	N_o
25	441.163	52.7	341.63	10.682	0.384432	2.5209	44
30	684	77.9	397.3	29.2857	3.81897	19.8076	27
40	1199	47.6	184.4	57.0582	2.8143	11.2537	16
50	1342	43.8	158.0	70.664	3.4465	12.8924	15
75	1381	21.1	76.0	76.6695	2.1083	7.8827	14
100	1402	18.5	64.2	78.5713	2.0588	7.42309	13

Resulting heartbeat outbursts modeled with different grids. First column N_p, gives the number of grid points. Last column, N_o, gives the number of outbursts in time interval of 20 ks

Parameters of model displayed on the animations

- Mass $6M_{\odot}$
- Wind parameter A between 0 and 100
- Accretion rate between 0.04 and 0.1 Eddington rate

Profile of density

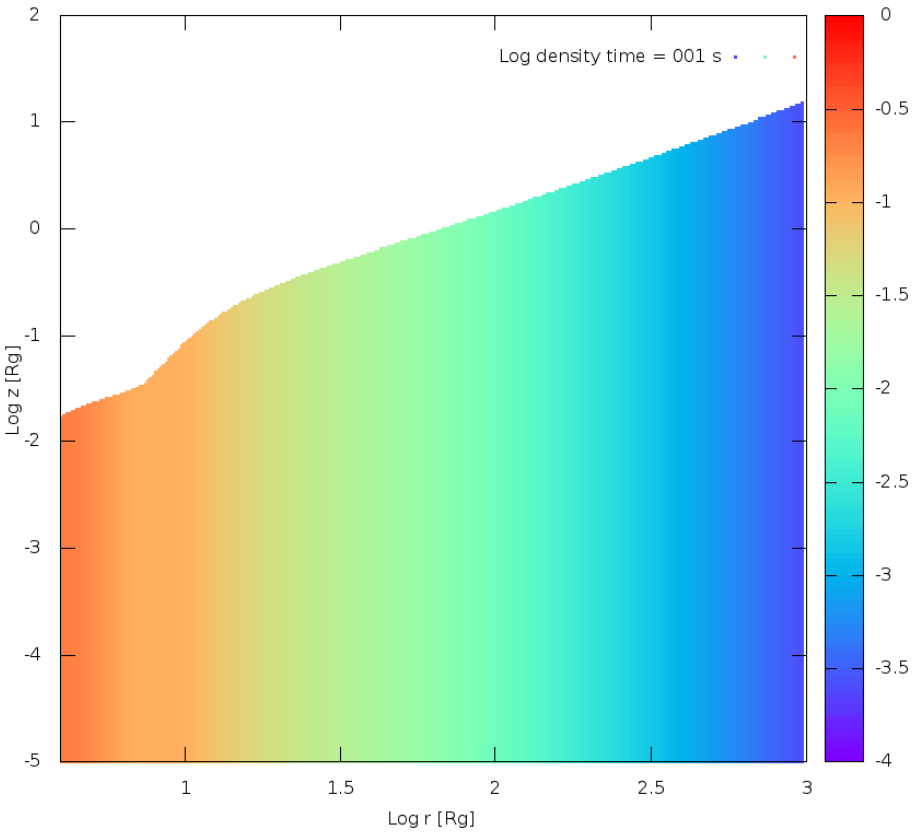

Profile of temperature

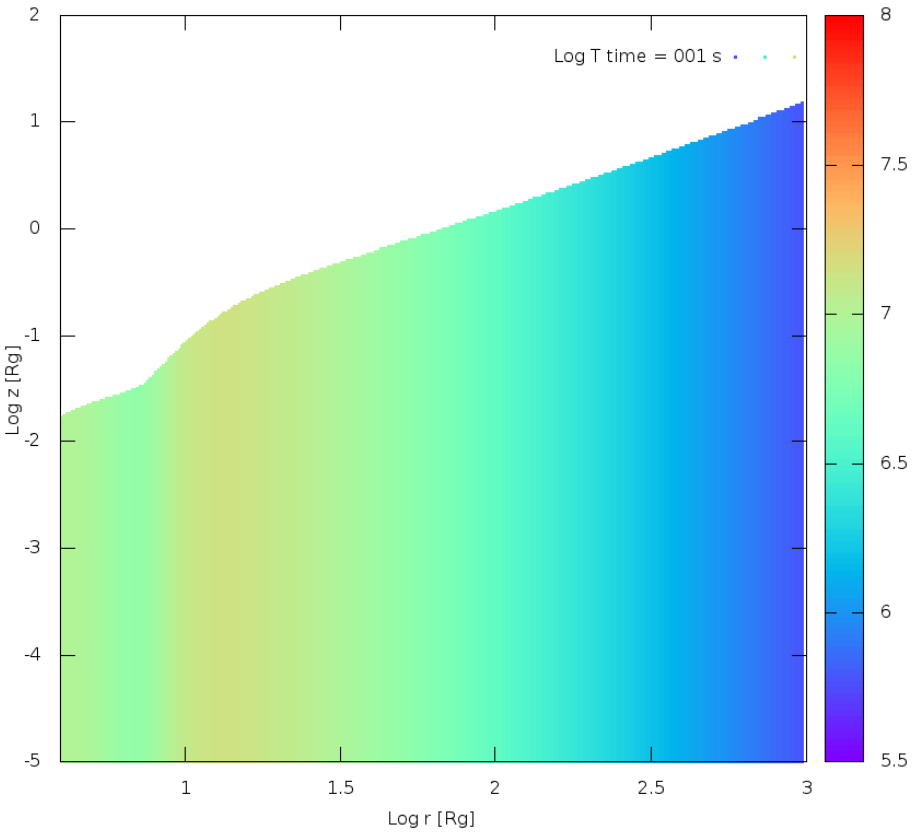

Grid of models

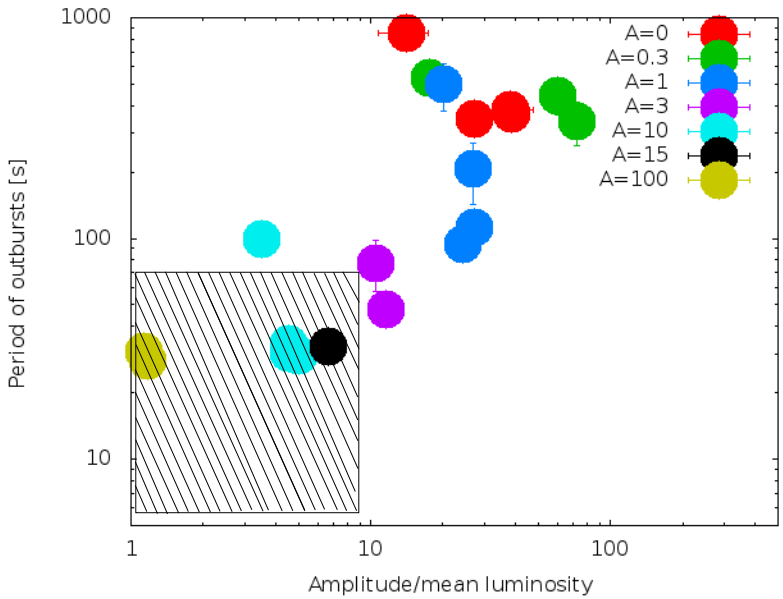

- Mass $6M_{\odot}$
- Wind parameter A between 0 and 100
- Accretion rate between 0.04 and 0.1 Eddington rate

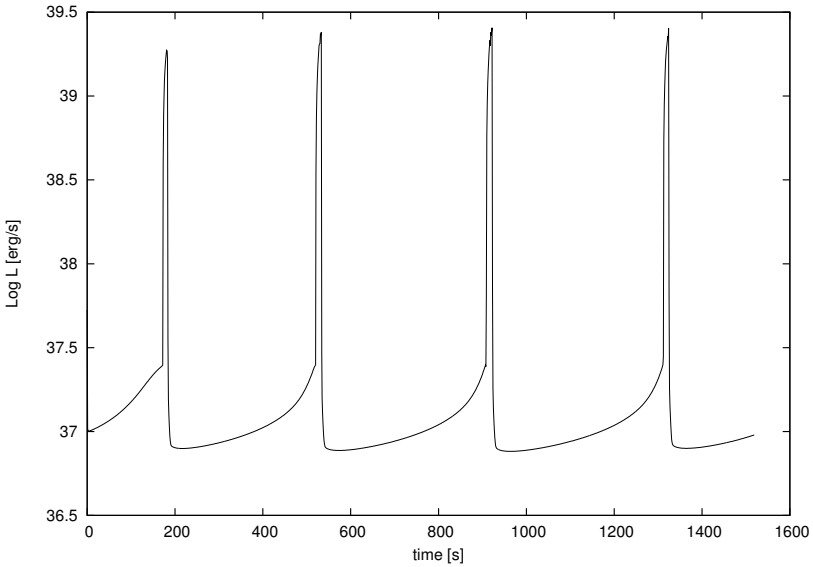

Figure: Lightcurve without wind

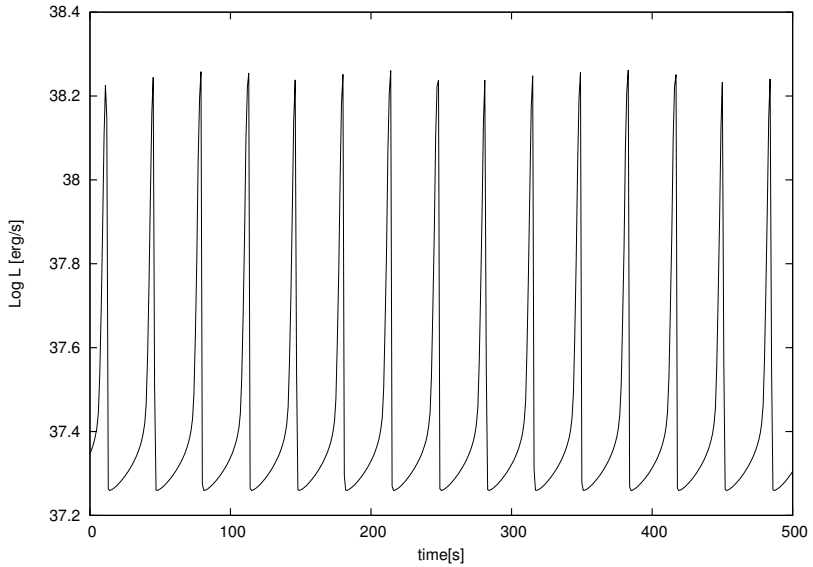

Figure: Lightcurve with wind

Mass loss

To obtain the total mass loss in the wind, we integrate $\dot{m}_z$ over the disk:

$$\Delta \dot{M}_{wind} = \int_{R_{min}}^{R_{max}} \dot{m}_z 4\pi r dr \tag{24}$$

We assumed diffetrent R_{min} and $R_{max} = 40000 R_{Schw}$ (for mass equal to 6 Solar masses, it gives $R_{max} = 7.08 \cdot 10^{11}$cm).
The actual mass loss will be on this order, or somewhat smaller, as the wind particles may be accelerated to obtain kinetic energy not necessarily equal to the virial energy, but rather to have a velocity a few (2-3) times their escape velocity at the radius r. Here we therefore may calculate the upper limit for the wind column density, depending on our model parameter A.

Mass loss and wind density

Value of wind mass loss is changing in time due to outbursts. Averaging the solutions, we obtain total mass loss caused by wind at the level of $\Delta \dot{M}_{wind} = 3 \times 10^{16} - 2 \times 10^{17}$ g/s.

Wind density

We calculate the wind density at R_{max}

$$\rho_{wind} = \frac{\dot{M}_{wind}}{4\pi R_{max}^2 v_{esc}} \tag{25}$$

where v_{esc} is the escape velocity at R_{max}. In our best-fit model, the density of the wind is equal between $\rho_{wind} = 2 \times 10^{-16}$ and gcm^{-3} and 7.2×10^{-16}

Column density of wind of protons

Assuming that wind consists of protons, we calculate the column density of the (spherically symmetric) wind:

$$\int \rho_{wind}(\vec{r})dr = \rho_{wind}(R_{max})R_{max}. \tag{26}$$

Observable column number density of particle is given by formula

$$N_H = \rho_{wind} R_{max} (f m_p)^{-1} \tag{27}$$

Where f is the filling factor in principle unknown and constrained from the observations of wind and we finally obtain the estimated value at the range between $N_H = 4.89 \cdot 10^{21}$ cm^{-2} and $1.62 \cdot 10^{22}$cm^{-2}

Model vs observation

- For the radii below $\sim$ 70 Schwarzschild radii, the dependence of $\dot{m}_Z(r)$ derived form Eq. (19) is a complicated function
- At larger radii it scales with radius as a simple power law with index -1.8.
- After integration we have:

$$\dot{M}_{\rm wind}(r, R_{\rm max}) = 1.635 \times 10^{16} (R_{\rm max}^{0.2} - r^{0.2}) \ [{\rm g\ s}^{-1}] \quad (28)$$

- First wind component with mass loss rate of about $\dot{M}_{\rm wind1} = 2.5 \times 10^{16}$ g s^{-1} with launching up to $R_{\rm max} \approx 4900 R_{Schw}$.
- The second wind component, with $\dot{M}_{\rm wind2} = 3.9 \times 10^{16}$ g s^{-1}, should be launched up to $R_{\rm max} \approx 5900 R_{Schw}$.

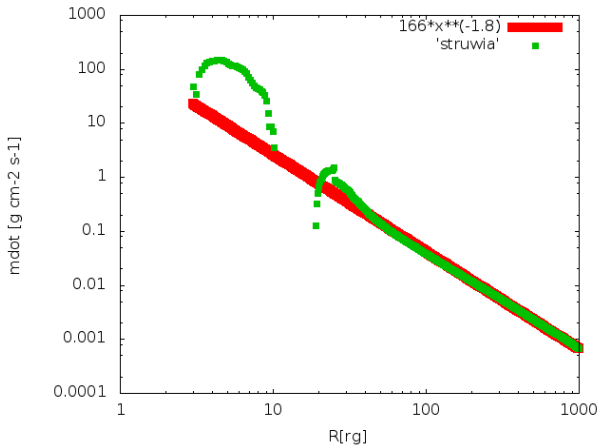

Model - Mass loss for different wind strength parameter

The resulting wind mass loss rate and density, for assumed wind strength parameter $A = 15$ and several values of accretion rate, are summarized in table below The column density is calculated assuming $f_1 = 0.0015$ wind extension $R_{\max} = 40000 R_g$.

R_{min}	$\dot{M}_{\rm wind}$ [g s^{-1}]	$\rho_{\rm wind}$ [g cm^{-3}]	$N_{\rm H}$ [cm^{-2}]
3	2.18×10^{17}	2.0×10^{-16}	5.66×10^{21}
70	8.84×10^{16}	3.9×10^{-16}	1.10×10^{22}
150	7.68×10^{16}	5.0×10^{-16}	1.07×10^{22}
350	6.04×10^{16}	7.1×10^{-16}	2.00×10^{22}
2000	3.06×10^{16}	7.2×10^{-16}	2.04×10^{22}

Wind parameter and disk stability

- With $A = 300$, a stable disk solution is found in our simulations, while the mass loss rate $\dot{M}_{\rm wind}$ is about ~ 12 times higher, than in the case of our heartbeat model with $A = 15$.
- Strong wind definitely stabilizes the heartbeat oscillations. There is a clear observable signature
- Taking the values of the wind velocities and mass loss rates such as those in the first *Chandra* observation, we obtain the observable wind laucching zones of $950 - 4200$ and $380 - 4700$ Schwarzschild radii, for the first and second wind component

Spectral modeling

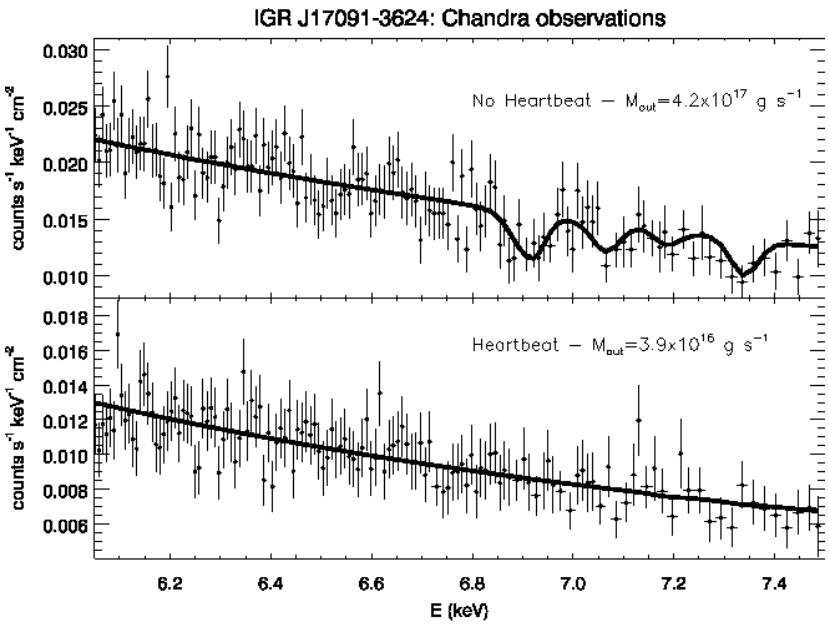

- Our wind density for accretion rate $\dot{m} = 0.1$ is included in the brackets of than results from the King et al., (2012), ApJL, 746, 20 obtained by spectral modelling
- Column density is modeled by the Fe absorption lines
- Fe XXV line 6.92 keV - outflow velocity 9300 km s^{-1}
- Fe XXVI line 7.32 keV - even higher velocity

Discussion

- Wind also exists in non-heartbeat and heartbeat states
- In hearbeat states is ten times fainter
- The mass outflow is 2.7 and 4.2×10^{17} g s^{-1} for the two wind components observed in the stable state, and about 2.5 and 3.9×10^{16} g s^{-1} in the heartbeat state.
- Wind ejection partially stabilized the disk
- There are two components of wind
- First component occurs between $\sim$ 380 and 4700-5900 $R_{\rm g}$
- Second component occurs between $\sim$ 950 and 4200-4900 Schwarzchild radii.
- Total mass loss rate $\dot{M}_{\rm wind}$ in these two components will be of the order of $\lesssim 4 \times 10^{16}$ g s^{-1} during the heartbeat oscilation
- In non-heartbeat states wind rate is $\lesssim 4 \times 10^{17}$ g s^{-1}

Our final conslusions are as follows:

- The heartbeat oscillations of the X-ray luminosity of IGR J17091 detected during its outburst in 2011 are attributed to the radiation pressure instability of the accretion disk
- The outflow launched from the disk on the cost of the part of the locally dissipated energy flux is plausible mechanism to regulate the amplitude of these oscillations
- The strong outflow may stabilize the disk and suppress the heartbeat completely

Our final conslusions are as follows:

- The observed properties of the wind detected from IGR J17091 in the state without the heartbeats allowed us to constrain the the mass loss rate at large distances in the disk
- The wind from the accretion disk, postulated by our model to stabilize the disk, is important in the innermost parts.
- In the spectroscopic observations, it may not always be detectable due to its high ionisation state or the velocities below the
- The MHD mechanism is rather driving the formation of a quasi-static, bound corona above the disk.
- We demonstrated that the observed winds are in good agreement with the scenario described by our model.

Thank you for attention